

## **Mechanism of Elongation of Gold or Silver Nanoparticles in Silica by Irradiation with Swift Heavy Ions**

Koichi Awazu<sup>1</sup>, Xiamin Wang<sup>1</sup>, Makoto Fujimaki<sup>1</sup>, Junji Tominaga<sup>1</sup>, Shinji Fujii<sup>2</sup>, Hirohiko Aiba<sup>2</sup>, Yoshimichi Ohki<sup>2</sup>, Tetsuro Komatsubara<sup>3</sup>

<sup>1</sup>CAN-FOR, National Institute of Advanced Science and Technology, 1-1-1 Higashi Tsukuba 305-8562, Japan; <sup>2</sup>Waseda University Shinjuku, Tokyo 169-8555, Japan; <sup>3</sup>Tandem Accelerator Complex, University of Tsukuba, Tsukuba 305-8577, Japan

### **Abstract**

It has been reported that elongated Au nanoparticles oriented parallel to one another can be synthesized in SiO<sub>2</sub> by ion irradiation. Our aim was to elucidate the mechanism of this elongation. We prepared Au and Ag nanoparticles with a diameter of 20 nm in an SiO<sub>2</sub> matrix. It was found that Au nanoparticles showed greater elongated with a higher flux of ion beam and with thicker SiO<sub>2</sub> films. In contrast, Ag nanoparticles split into two or more shorter

nanorods aligned end to end in the direction parallel to the ion beam. These experimental results are discussed in the framework of a thermal spike model of Au and Ag nanorods embedded in SiO<sub>2</sub>. The lattice temperature exceeds the melting temperatures of SiO<sub>2</sub>, Au and Ag for 100 ns after one 110-MeV Br<sup>10+</sup> ion has passed through the middle of an Au or Ag nanorod.

Author to whom correspondence should be addressed. Electronic mail: [k.awazu@aist.go.jp](mailto:k.awazu@aist.go.jp)

PACS: 81.16.-c, 61.80.Jh, 62.20.Fe, 81.40.Lm, 68.60.Bs

Key words; swift heavy ion, nanofabrication, Au nanoparticles, silica glass

## 1. Introduction

Well-defined Au nanoparticles and nanorods are desirable for their optical properties. The size and shape of nanocrystals affect the position of the plasmon bands, which in turn have been widely used in surface enhanced spectroscopy that includes both Raman and fluorescence. Gold nanoparticles or nanorods can be deposited randomly on a substrate,[1] but it is difficult to synthesize Au nanorods that are oriented parallel to each other and perpendicular to the substrate.[2], [3] The goal of the experiment from the viewpoint of

application to nanophotonics was to reveal new optical properties of Au nanorods. We also aimed to resolve the interesting phenomenon of elongation of Au nanoparticles in SiO<sub>2</sub>. To theoretically understand the mechanism of elongation, we employed the thermal spike model,[4] since it explains many phenomena caused by ion bombardment. However, several problems with thermal spike models have been pointed out.[5] For example, temperature changes in the order of femto-seconds cannot be defined. It is also impossible to ignore the pressure dependence of the different physical parameters of the lattice. Such questions remain controversial, so we will not focus on these matters in the present report.

## 2. Experimental procedures

A thermally oxidized silicon wafer was prepared as the SiO<sub>2</sub> substrate. The thickness of the SiO<sub>2</sub> layer on the silicon was 2 μm. Five-nm-thick Au or Ag films were deposited on the substrate by evaporation of high-purity Au or Ag grains. After deposition, both the thin Au and Ag films were heated at 300 °C for 10 min to form nanoparticles. The nanoparticles were then embedded in an SiO<sub>2</sub> layer deposited by radio frequency magnetron sputtering of a silica

target in an Ar atmosphere. The thickness of the top layer of SiO<sub>2</sub> was set to 200 nm or 1 μm by selecting deposition time. The direction of propagation of the ion beam was perpendicular to the upper surface of the SiO<sub>2</sub>. The 12-unit double-Pelletron tandem accelerator at the University of Tsukuba was used to irradiate the assemblies with 110-MeV Br<sup>10+</sup> ions. Cross-sections of the pristine and irradiated samples were examined by transmission electric microscopy (TEM) using a Hitachi H-9500 300-kV instrument. Specimens for TEM observation with a thickness of 100 nm were produced using a focused beam of 20-keV Ga<sup>+</sup> ions from a Hitachi FB-2100 instrument.

The temperature evolutions of the particles when irradiated by swift heavy ions are simulated using the thermal spike model [4,7,8]. We extended this model to include two materials to accommodate the current particle case. First, the swift ion deposits its energy in the electron subsystem according to the radial distribution given by the Katz model [9]. The hot electrons then diffuse their energy by means of electron-electron scattering and electron-phonon coupling. To simulate this heat-diffusing process numerically, we need to know all the thermal parameters. For the electron subsystems' specific heats and thermal conductivities, we assumed constant values for the insulator SiO<sub>2</sub> as given in [4] and temperature-dependent

values for the metal Au and Ag as in [8]. For the lattice subsystems, we used the thermodynamic parameters of bulk materials as an approximation. SiO<sub>2</sub>'s specific heat is fitted to the data given by [10, 11], and the specific heats of Au and Ag are from [12]. Their thermal conductivities are from the data recommended in Touloukian's handbook [13]. In addition, the electron-lattice coupling parameter of SiO<sub>2</sub> is derived from the experimentally fitted mean energy diffusion length  $\lambda$  given by [4]. The coupling parameter of silver is given theoretically by the quasi-free electron gas model [8].

### 3. Results and discussion

We examined the elongation of Au nanoparticles as a function of the thickness of SiO<sub>2</sub> on Au nanoparticles and as a function of ion flux. Figures 1 show cross-sectional TEM views of Au nanoparticles generated at 300 °C and subsequently embedded in SiO<sub>2</sub>. The thicknesses of the SiO<sub>2</sub> layer for Au nanoparticles in (a), (b) and (d) are 200 nm and for (c) it is 1  $\mu$ m.

Figure 1 (a) presents Au nanoparticles in SiO<sub>2</sub> before irradiation. Particle size is estimated from the TEM view at 20 nm. The Au particles in the pristine film seems to be touching each other in Figures 1 (a). But from plane view of scanning electronic microscope (SEM), we

confirmed that Au particles were separated. Figures 1(b), (c) and (d) show Au nanoparticles embedded in SiO<sub>2</sub> after irradiation with 110-MeV Br<sup>10+</sup> ions at a fluence of  $1 \times 10^{14} \text{ cm}^{-2}$ . Ion fluxes are  $8 \pm 2 \times 10^{10} \text{ cm}^{-2} \text{ sec}^{-1}$  for (b) and (c) and  $1.5 \pm 0.2 \times 10^{11} \text{ cm}^{-2} \text{ sec}^{-1}$  for (d). In the pictures, the direction of ion propagation is from top to bottom, as shown by the arrow. A comparison between (b) and (d) shows that Au nanoparticles under 1  $\mu\text{m}$  thick SiO<sub>2</sub> were much more elongated than those under 200 nm thick SiO<sub>2</sub>. A comparison between (b) and (c) reveals that Au nanoparticles are much more elongated at higher ion fluxes.

Here we discuss the dependence of SiO<sub>2</sub> thickness. Kläumunzer et al. proposed the effect of matrix hammering introduced the particles creep.[14] Penninkhof et al. have reported that in colloids consisting of a Au core and a silica shell, the Au core showed a large elongation along the ion beam direction, provided the silica shell is thick enough (>40nm). [15] Our present results are consistent with the report by Penninkhof et al.. The model proposed by them to explain the elongation of the Au core is an indirect deformation scenario in which the in-plane strain generated by ion tracks in the silica shell imposes a stress on the metal core. [15] With the Au being relatively soft under ion irradiation, this in-plane stress may then cause the Au core to flow in the out-of-plane direction, i.e. along the direction of the

ion beam, by Newtonian viscous flow. [15] This argument seems consistent with the fact that larger elongation is found for colloids with a thicker silica shell. About the flux dependence, we assumed that at high flux they did not have the time to cool between successive impacts on the same area.

Silver nanoparticles embedded in SiO<sub>2</sub> are shown in Figure 2 (a). The thickness of the top layer of SiO<sub>2</sub> is 200 nm. Ag nanoparticles of a uniform diameter of 20 nm are present in the SiO<sub>2</sub>. After irradiation with 110-MeV Br<sup>10+</sup> ions at a fluence of  $1 \times 10^{14} \text{ cm}^{-2}$  and at a flux of  $8 \pm 2 \times 10^{10} \text{ cm}^{-2} \text{ sec}^{-1}$ , Ag nanoparticles split into two or more shorter nanorods aligned end to end in the direction parallel to the ion beam.

Penninkhof et al. reported the behavior of Ag cores embedded in silica with 30MeV Si ions irradiation and Ag cores did not show elongation. [15] The Ag behavior in the present work is different from the previous report.

Lattice temperature for Au and Ag nanorods with radii of 5 nm embedded in SiO<sub>2</sub> were calculated and are shown in Figures 3 (a) and (b), respectively. Here we used nanorods, not nanoparticles because calculation of temperature on nanorods is simpler than that on nanoparticles and Au shape is close to nanorods after irradiation. These show the evolution of

the lattice temperature against time at various distances from the ion axis. For a time of less than  $10^{-13}$  s, the temperature characterizes the energy imparted to the atoms. In Figure 3(a), the temperatures of the Au nanorod monitored at 1 nm and 3.5 nm from the center are shown by black squares and red circles, respectively. 300 fs ( $3 \times 10^{-13}$  s) after the ion impact, both temperatures exceed the melting point of Au (1337 K), which is shown by a black dashed line. The maximum temperatures at both distances also reach the melting point of  $\text{SiO}_2$  (1992 K), which is shown by a dashed horizontal line. A point 6.5 nm from center of an Au nanorod of radius 5 nm is located within the  $\text{SiO}_2$  matrix. The temperature there at this point increases dramatically 5 fs ( $5 \times 10^{-15}$  s) after ion impact, and exceeds the melting point of  $\text{SiO}_2$  for a period between 20 fs and 10 ps after the ion impact. The lattice temperature 10 nm from the center of the nanoparticle does not exceed the melting point of  $\text{SiO}_2$ .  $\text{SiO}_2$ , as well as Au, is melted for 10 ps in the region within 10 nm of the center of the nanoparticle. In other words, the periphery of particles rather undergo an overheating with respect to the core because of the low thermal conductivity of the surrounding matrix.

Here we should explain why the silica temperature increases before that of the Au nanoparticle even though the incident ion energy is first deposited in the Au nanoparticle and

only then coupled to the silica matrix. The electrons along the ion's path respond instantaneously to the penetrating ion, resulting in a rise in electronic temperature. These hot electrons within Au then diffuse their energy rapidly to electrons in the surrounding silica and cause their temperature to be raised correspondingly. Because the electron-lattice coupling constant of silica is greater than that of Au although its conductivity is smaller, we observed in the simulation that the silica lattice temperature increases ahead of the inner Au particle, and thus will feed the heat back to the particle by phonon-phonon interactions.

In the experiment, however, Au nanoparticles 10 nm in radius are elongated by irradiation from the experimental results as depicted in Figure 1. The radius in the experiments does not exactly match those obtained in the calculation, due to the inherent limitations of the current spike model as well as uncertainty of the input parameters.

We found from Figures 1 (b) and (d) that the elongation of Au nanoparticles depends on ion flux. This may imply that cooling time is not sufficient after initial ion bombardment at higher ion flux. It was found that Au nanoparticles are elongated but that Ag nanoparticles are split into two or more. Figures 3 (a) and (b) based on the thermal spike mode reveal no obvious difference in the lattice temperatures of Au and Ag nanoparticles in SiO<sub>2</sub>.

## Summary

In the present study, we found that the elongation of Au nanoparticles embedded in SiO<sub>2</sub> was influenced by ion flux and SiO<sub>2</sub> thickness. Silver nanoparticles are elongated and split into two or more under irradiation. We concluded that the elongation mechanisms must consist of combination of the particle creep under the effect of the matrix hammering, thermal spike, mechanical effects driven by stresses around the ion tracks.

Acknowledgement: This study was financially supported by the Budget for Nuclear Research of the Ministry of Education, Culture, Sports, Science, and Technology, based on screening and counseling by the Atomic Energy Commission.

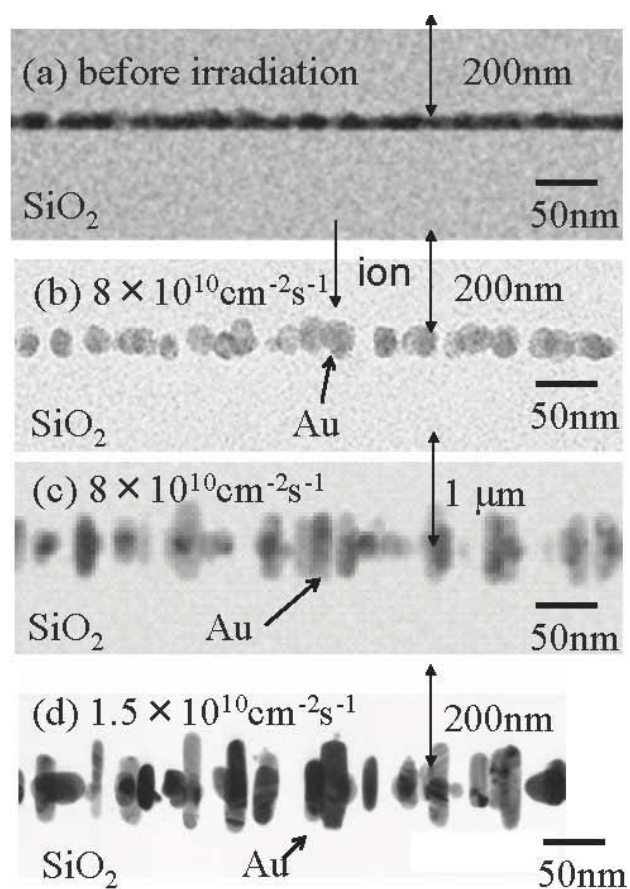


**Figure 1** Cross-sectional TEM image of Au nanoparticles embedded in SiO<sub>2</sub>. (a), before ion irradiation. (b)-(d), irradiated with 110-MeV Br<sup>10+</sup> at a fluence of  $1 \times 10^{14} \text{ cm}^{-2}$ . Thicknesses of SiO<sub>2</sub> are 200 nm [(a), (b), (d)] and 1  $\mu\text{m}$  (c). Ion fluxes are  $8 \pm 2 \times 10^{10} \text{ cm}^{-2} \text{ sec}^{-1}$  [(b), (c)] and  $1.5 \pm 0.2 \times 10^{11} \text{ cm}^{-2} \text{ sec}^{-1}$  (d).

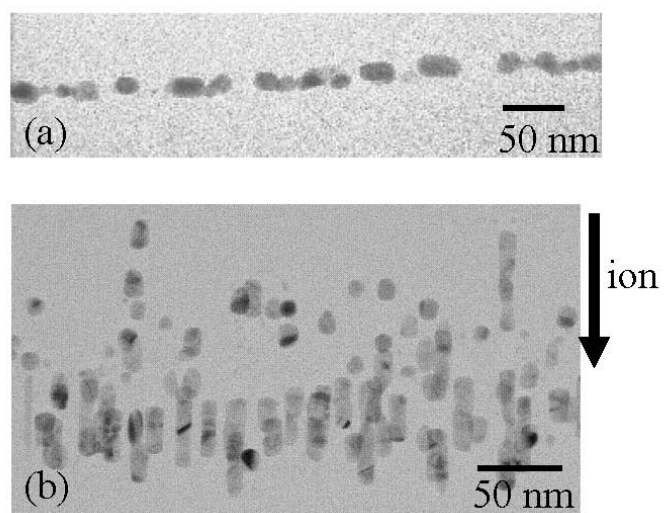


**Figure 2** Cross-sectional TEM image of Ag nanoparticles embedded in SiO<sub>2</sub>. (a) followed by 110-MeV Br<sup>10+</sup> ion bombardment at a fluence of  $1 \times 10^{14} \text{ cm}^{-2}$  and at a flux of  $8 \pm 2 \times 10^{10} \text{ cm}^{-2}$ .

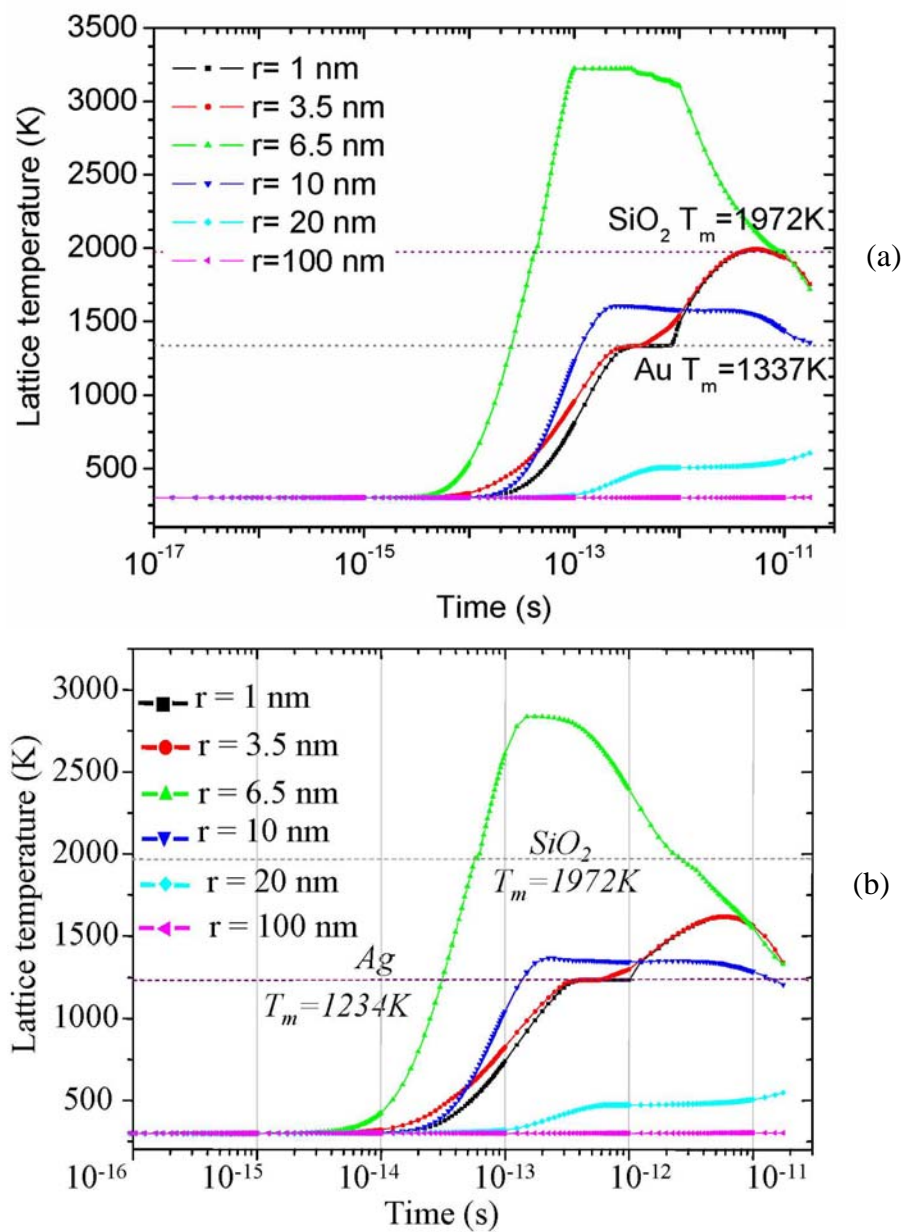


**Figure 3** The calculated lattice temperature versus time at distances of 1, 3.5, 6.5, 10, 20, and 100 nm from the ion path. (a) and (b), 5-nm-radius Au and Ag nanoparticles embedded in SiO<sub>2</sub>, respectively. The sample is at 300 K. The melting temperatures of SiO<sub>2</sub>, Au and Ag are shown in the Figures.

## Reference

- [1] N. Halas, *MRS Bull.*, 30 (2005) 362.
- [2] S. Roorda, T. V. Dillen, A. Polman, C. Graf, A. V. Blaaderen and B. J. Kooi, *Adv. Mater.*, 16 (2004) 235.
- [3] Y. K. Mishra, D. K. Avasthi, P. K. Kulriya, F. Singh, D. Kabiraj, A. Tripathi, J. C. Pivin and I. S. Bayer, A. Biswas, *Appl. Phys. Lett.* 90 (2007) 073110.
- [4] M. Toulemonde, E. Paumier, J.M. Costantini, Ch. Dufour, A. Meftah and F. Studer, *Nucl. Instrum. and Methods*, B116 (1996) 37.
- [5] S. Klaumünzer, *Matematisk-fysiske Meddelelser* 52 (2006) 293.
- [6] S. Eustis and M. A. El-Sayed, *Chem. Soc. Rev.*, 35 (2006) 209.
- [7] M. Toulemonde, C. Dufour, A. Meftah and E. Paumier, *Nucl. Instrum. and Methods*, B166 (2000) 903.

[8] Z. G. Wang, C. Dufour, E. Paumier and M. Toulemonde, *J. Phys.: Condens. Matter*, 6 (1994) 6733.

[9] M. P. R. Waligorski, R. N. Hamm and R. Katz, *Radiation Measurements*, 11 (1986) 309.

[10] David R. Lide (Editor), *CRC Handbook of Chemistry and Physics - A Ready-Reference Book of Chemical and Physical Data*, 86th Edition (CRC Press, Boca Raton, 2006).

[11] R.H. Perry and D. W. Green, *Perry's Chemical Engineers' Handbook*, the sixth edition, McGraw-Hill Book (New York, 1984).

[12] HSC Chemistry for Windows, Ver. 5.1, ESM Software (2005).

[13] Y. S. Touloukian, R. W. Powell and C. Y. Ho, et al (ed), *Thermophysical Properties of Matter*, 1 (IFI/Pleum , New York , 1970) 132.

[14] S. Klaumünzer, C.L. Li, S. Löffler, M. Rammensee, G.Schumacher and H.C. Neitzer, *Rad. Eff. and Def. Sol.* 108 (1989) 131.

[15] J.J. Penninkhof, T.van Dillen, S. Roorda, C. Graf, A. van Blaaderen, A. M. Vredenberg and A. Polman, *Nucl. Instr. and Met. in Phys. Res.* B242 (2006) 523.